

A Wide-Temperature-Range, Low-Cost, Fluorine-Free Battery Electrolyte Based On Sodium Bis(Oxalate)Borate

Ronnie Mogensen, Alexander Buckel, Simon Colbin, and Reza Younesi*



Cite This: *Chem. Mater.* 2021, 33, 1130–1139



Read Online

ACCESS |



Metrics & More

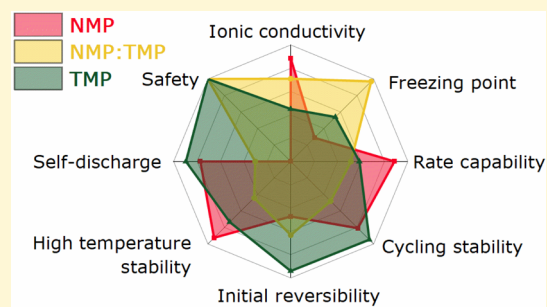


Article Recommendations



Supporting Information

ABSTRACT: Common battery electrolytes comprise organic carbonate solvents and fluorinated salts based on hexafluorophosphate (PF_6^-) anions. However, these electrolytes suffer from high flammability, limited operating temperature window, and high cost. To address those issues, we here propose a fluorine-free electrolyte based on sodium bis(oxalate)borate (NaBOB). Although lithium bis(oxalate)borate (LiBOB) has previously been investigated for lithium-ion batteries, NaBOB was considered too insoluble in organic solvents to be used in practice. Here, we show that NaBOB can be dissolved in mixtures of *N*-methyl-2-pyrrolidone (NMP) and trimethyl phosphate (TMP) and in each sole solvent. NMP provides higher solubility of NaBOB with a concentration of almost 0.7 M, resulting in an ionic conductivity up to 8.83 mS cm^{-1} at room temperature. The physical and electrochemical properties of electrolytes based on NaBOB salt dissolved in NMP and TMP solvents and their binary mixtures are here investigated. The results include the thermal behavior of the sole solvents and their mixtures, flammability tests, NaBOB solubility, and ionic conductivity measurements of the electrolyte mixtures. Full-cell sodium-ion batteries based on hard carbon anodes and Prussian white cathodes were evaluated at room temperature and 55°C using the aforementioned electrolytes. The results show a much improved performance compared to conventional electrolytes of 1 M NaPF_6 in carbonate solvents at high currents and elevated temperatures. The proposed electrolytes provide a high ionic conductivity at a wide temperature range from room temperature to -60°C as NMP–TMP mixtures have low freezing points. The flammability tests indicate that NaBOB in NMP–TMP electrolytes are nonflammable when the electrolyte contains more than 30 vol % TMP.



INTRODUCTION

Sodium-ion batteries are in many aspects similar to lithium-ion batteries and often stated as the technology that will be used in the large-scale storage segment of the battery market due to their potential to decrease costs.^{1–3} The abundance and low cost of raw materials are the underlying arguments for such statements, and although it is potentially true for electrode materials based on naturally abundant elements such as iron, manganese, and carbon, it is not as clear cut for electrolytes.^{4,5} The perceived necessity of common expensive electrolyte salts, such as sodium salts based on hexafluorophosphates (PF_6^-) or even more costly salts like bis(fluorosulfonyl)imid (FSI^-) or bis(trifluoromethanesulfonyl)imide (TFSI^-), presents a bottleneck in an attempt to decrease the cost of electrolytes for sodium-ion batteries.⁶

Bis-oxalato borate (BOB^-) is an alternative anion that has been extensively studied for lithium-ion batteries,^{7–9} but it has only recently been investigated in sodium-ion batteries.¹⁰ Lithium bis(oxalate)borate (LiBOB) has shown to be a cost-effective salt with many attractive properties in terms of passivation of both graphite and aluminum.^{11,12} Therefore, LiBOB has become a popular component in electrolytes that aims to lower the fluorine content while increasing stability in electrolytes based on carbonates,^{13–15} lactones,¹⁶ and sulfones.¹⁷ Furthermore, the strong passivating properties of

LiBOB in traditional solvents also seem to persist when it is used in conjunction with nonflammable solvents like trimethyl phosphate (TMP) and dimethyl methyl phosphonate (DMMP).^{18–20}

Sodium bis(oxalate)borate (NaBOB) however has not received much attention after its synthesis was reported by Whittingham *et al.*²¹ since it was deemed insoluble in any common solvents such as carbonates and acetonitrile. NaBOB has shown slight solubility in DMF,²² but so far, only TMP–NaBOB has been reported to achieve practical ionic conductivity and actual cell cycling.¹⁰

Here, we demonstrate for the first time that an NMP (*N*-methyl-2-pyrrolidone) solvent can dissolve a relatively high amount of NaBOB (0.66 M), resulting in a higher ionic conductivity (8.83 mS cm^{-1}) than EC:DEC 1 M NaPF_6 (6.44 mS cm^{-1}).²³ NMP might appear to be an odd choice as an

Received: September 4, 2020

Revised: January 19, 2021

Published: February 9, 2021



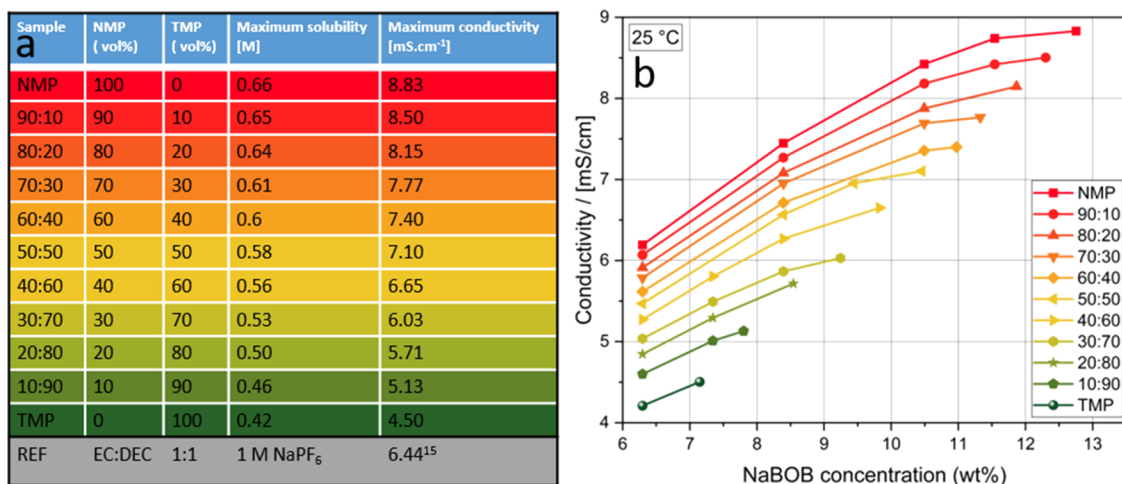


Figure 1. Samples list with solvent composition, maximum salt concentration, and maximum ionic conductivity at room temperature (a) and ionic conductivity of the electrolytes at room temperature as a function of NaBOB concentration in the binary mixtures (b).

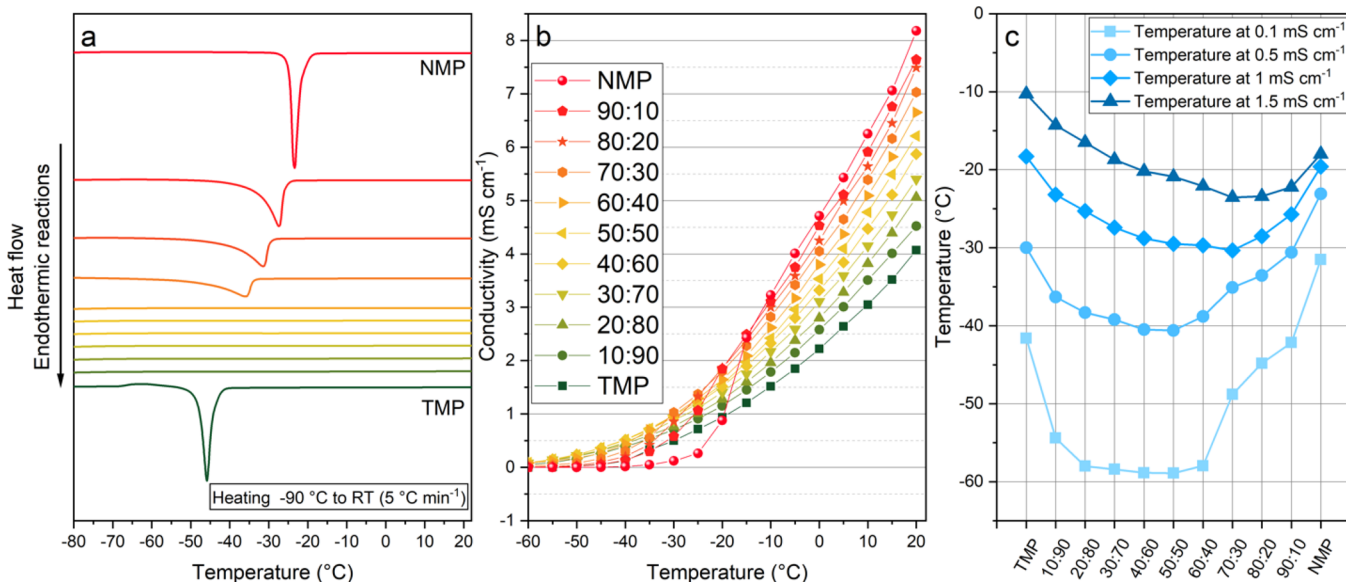


Figure 2. DSC measurements of salt-free solvent mixtures showing the first heating scan after cooling to $-90\text{ }^{\circ}\text{C}$ with a scan speed of $5\text{ }^{\circ}\text{C}/\text{min}$ for both heating and cooling scans (a). Conductivity measurements at low temperature on samples using the NaBOB concentration corresponding to their maximum room-temperature ionic conductivity (b) and temperature threshold values for 0.1, 0.5, 1, and $1.5\text{ mS}\cdot\text{cm}^{-1}$ of the same samples (c).

electrolyte solvent due to its bad reputation for being flammable and toxic, but we view NMP as a good model solvent that can be substituted by a number of similar and more benign solvents. We also display that NMP–TMP mixtures can easily become nonflammable while preserving promising electrochemical performance in full-cell sodium-ion batteries based on hard carbon anodes and Prussian white cathodes.

Earlier efforts directed at lowering the cost and improving safety of the electrolytes in sodium-ion batteries include the use of NaBF_4 in tetraethylene glycol dimethyl ether electrolyte shown by Balaya *et al.*²⁴ Although the proposed approach achieved a nonflammable and low-cost electrolyte, the electrolyte provides a rather low ionic conductivity of $1.3\text{ mS}\cdot\text{cm}^{-1}$, which is barely above the minimum practical conductivity (>1 to $2\text{ mS}\cdot\text{cm}^{-1}$).²⁵ Other studies with similar aims proposed TMP-based^{23,26–28} and TEP-based²⁹ electrolytes using either NaPF_6 , NaClO_4 , or NaFSI , and although many of those electrolyte formulations show promise, TMP-based electrolytes are not

compatible against hard carbon unless very high concentrations of salt or electrolyte additives are used. The main drawbacks of the highly concentrated electrolytes are high cost and low conductivity. For example, electrolytes consisting of 3.3 M NaFSI in TMP or 2.5 M NaClO_4 in TMP achieve an ionic conductivity of 2.2 or $2.35\text{ mS}\cdot\text{cm}^{-1}$, respectively.^{27,28} Another main strategy employed to reduce flammability has been to add fluorinated solvents such as 1,1,2,2-tetrafluoroethyl-2,2,3,3-tetrafluoropropyl ether (F-EPE). Addition of fluorinated solvents to electrolytes can enable nonflammability combined with decent ionic conductivity, as demonstrated by Cao,³⁰ who achieved good results using a 2:1 ratio of TMP–F-EPE with 2 M NaPF_6 and $2\text{ wt}\%$ FEC with an ionic conductivity of $4.67\text{ mS}\cdot\text{cm}^{-1}$. However, those highly fluorinated electrolytes are subject to health concerns, especially the fluorinated carbon chains that have been shown to bio-accumulate in nature and the human body.⁹

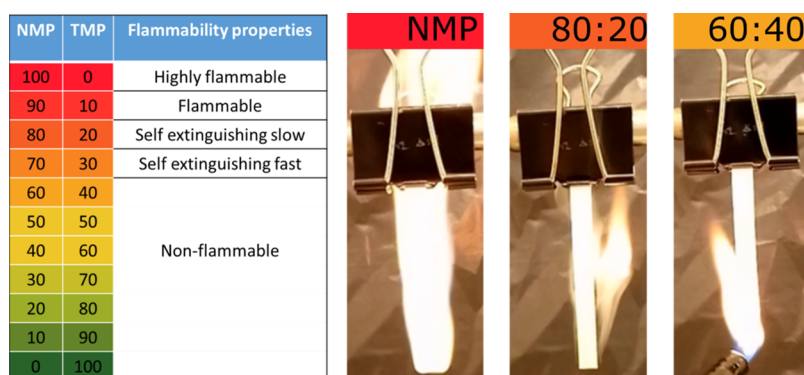


Figure 3. Flammability tests with three pictures showing frames from video recordings of tests conducted on NMP, 80:20 NMP–TMP, and 60:40 NMP–TMP electrolyte samples.

Therefore, our proposed electrolytes are based on NaBOB salt and mixed solvents of TMP and NMP with promising physical properties as being nonflammable electrolytes with high ionic conductivity without per- and polyfluoroalkyl substances (PFAS). Furthermore, the electrolytes yield promising electrochemical results for long-term cycling of sodium-ion full cells at room and high temperature, and it is a significant step toward a low-cost alternative to heavily fluorinated or high-concentration electrolytes.

RESULTS AND DISCUSSION

To map the NMP–TMP solvent system, eleven samples were first prepared ranging from NMP to TMP as the sole solvents with 10 vol % increments to prepare the binary solvent mixtures. These mixtures are here denoted as X:Y where X represents the vol% of NMP and Y indicates the vol % of TMP (see Figure 1a). We found that the two solvents are fully miscible and that they produced a clear homogeneous liquid. Pure TMP can dissolve up to 0.42 M (7.2 wt %) NaBOB, while pure NMP was close to saturation at 0.66 M (12.8 wt %) NaBOB. For the intermediate samples, there was a clear correlation between increased solubility and NMP content. The solubility presented herein was achieved by simple stirring, and we recognize that higher concentrations of the salt are probably feasible if heating and long-time scales are used for the dissolution of the salt.

The conductivity of the whole series was measured as a function of NaBOB concentration at room temperature (see Figure 1b). The results show that both NMP and TMP as well as the solvent mixtures all achieve their maximum conductivity at their maximum concentration. NaBOB–TMP reached $4.5 \text{ mS}\cdot\text{cm}^{-1}$, while NaBOB–NMP attained $8.83 \text{ mS}\cdot\text{cm}^{-1}$, which is higher than the ionic conductivity of the “standard” electrolyte 1 M NaPF₆ in EC:DEC that is reported to reach $6.44 \text{ mS}\cdot\text{cm}^{-1}$.²³ The electrolytes based on mixtures of NMP–TMP had intermediate values that increased with the amount of NMP and thus concentration of NaBOB.

In regard to solvent properties, both TMP and NMP have very low vapor pressures and quite wide liquid ranges, where TMP has a low freezing point of $-46 \text{ }^\circ\text{C}$ ³¹ and boiling point of $197 \text{ }^\circ\text{C}$ while NMP has a higher freezing point of $-25 \text{ }^\circ\text{C}$ ³² but a similar boiling point of $202 \text{ }^\circ\text{C}$.³³ Differential scanning calorimetry (DSC) was used to assess freezing points of the salt-free solvent mixtures. The melting point of NMP decreased upon addition of TMP, and this coincided with a significant shift in the onset of the melting peak toward lower temperatures (Figure 2a). The shift in the onset of the melting peak from

100% to 70% NMP combined with the lack of melting peaks in the compositional range of 60% NMP to 10% NMP indicates that this region contains a composition that is either amorphous or has a very low melting point. The full DSC scans are presented in the Supporting Information (Figure S1).

Conductivity measurements of all samples with the maximum concentration of NaBOB were determined between -80 and $20 \text{ }^\circ\text{C}$ to investigate the low-temperature behavior of the electrolytes. The results presented in Figure 2b disclose that a pure NMP electrolyte has a steep increase in conductivity at roughly $-30 \text{ }^\circ\text{C}$ and above, which most likely coincides with the melting point of NMP containing 0.66 M NaBOB. For the NaBOB–TMP electrolyte, the increase in the conductivity was much less distinct and started at ca. $-45 \text{ }^\circ\text{C}$. All mixtures containing between 60 and 90 vol % TMP showed significantly higher ionic conductivities below $-20 \text{ }^\circ\text{C}$ than the single solvent electrolytes, and their ionic conductivity started to increase close to $-60 \text{ }^\circ\text{C}$ with somewhat practical conductivities ($1 \text{ mS}\cdot\text{cm}^{-1}$)²⁵ being achieved as low as $-30 \text{ }^\circ\text{C}$ (see Figure 2c).

The effects of mixing the flame-retardant TMP with the flammable NMP were investigated by a simple test using solvent-soaked glass fiber strips and a butane lighter (Figure 3 and supplementary videos in the Supporting Information). The electrolyte samples tested contained NaBOB in concentrations corresponding to their maximum conductivity. All mixtures that contained 60 vol % or less NMP showed no signs of burning, while the mixtures using 70 or 80 vol % NMP could be temporarily ignited, but without a self-sustaining flame. The pure NaBOB–NMP burned with vigor, and although the electrolyte containing 10 vol % TMP was clearly flammable, it was less than the pure NaBOB–NMP electrolyte. The true properties of flammability are hard to confer in a text or picture format, and therefore, the tests were filmed and the videos are available in the Supporting Information. The experiments performed by Wang *et al.*²⁸ showed that the vapors of dimethyl carbonate (DMC) can be ignited when 1:1 mixtures of TMP–DMC are heated. This indicates that further testing needs to be conducted to get accurate determination of the safety level of any mixture of TMP and a volatile solvent. That being said, NMP and DMC have very different vapor pressures at 25 and 7400 Pa at $25 \text{ }^\circ\text{C}$, respectively.

Electrochemical Stability. The electrochemical stability of the NaBOB–50:50 electrolyte as well as the pure NaBOB–NMP and NaBOB–TMP electrolytes was measured by cyclic voltammetry. The electrolytes used their respective maximum concentrations of NaBOB, and separate cells were used for

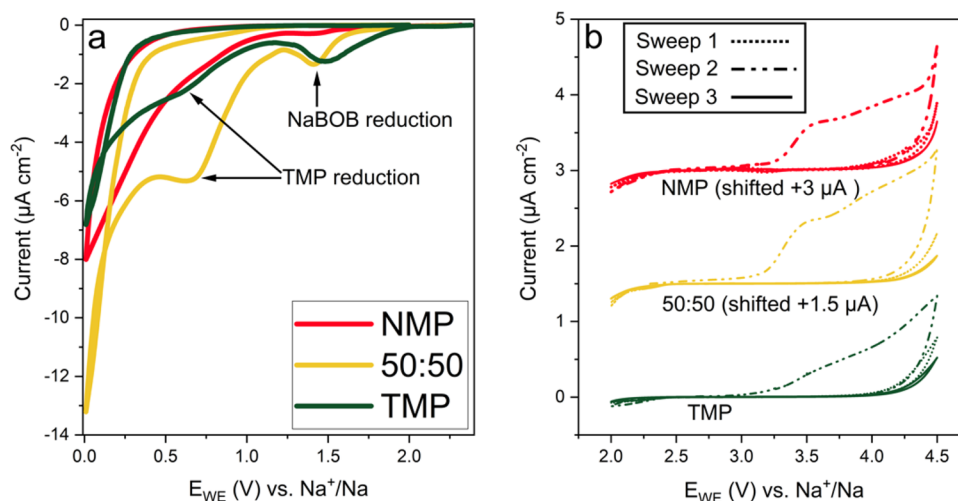


Figure 4. First reduction scan (a) and the first three oxidation scans (b) for 0.66 M NMP, 0.58 M 50:50, and 0.42 M TMP electrolytes. The scan speed $0.1 \text{ mV}\cdot\text{s}^{-1}$ was applied for all the cells, and a three-electrode setup using a PW reference electrode was used.

oxidation and reduction scans. The results in Figure 4a show that the first reduction peak, herein ascribed to NaBOB reduction, was observed for all electrolytes starting roughly at $2 \text{ V vs Na}^+/\text{Na}$ and the TMP-based electrolyte seemed to consume more NaBOB than the NMP-based electrolyte. The reduction of NaBOB in the NMP-based electrolyte was slightly shifted to more reducing potentials; however, TMP-based and 50:50 electrolytes had roughly the same reduction peak position with similar currents. A second reduction peak was visible for TMP-containing electrolytes at 0.7 V , suggesting that TMP is being reduced, although the 50:50 electrolyte showed a higher current than the single solvent electrolytes. The voltage profiles during the SEI formation in the galvanostatic cycling reveal that between 10 and 20% of the charge capacity was consumed during the initial formation (see Figure S2). Interestingly, the galvanostatic voltage profiles from cells with hard carbon anodes indicate that electrolytes that contained a majority of NMP decomposed at a higher potential than 50:50 mixtures and TMP-based electrolytes. CVs using sodium metal reference electrodes and aluminum working electrodes also indicate that NMP is reduced at higher potentials than TMP (see Figure S3).

Figure 4b displays the oxidation behavior of the three electrolytes that were studied over three consecutive oxidation sweeps. All electrolytes showed a moderate oxidation current during the first sweep that is significantly reduced by the third sweep. The upper potential stability limit after passivation was ca. $4 \text{ V vs Na}^+/\text{Na}$ for all the electrolytes. The nature of this passivation is unknown, although studies on LiBOB suggest that formation of AlBO_3 occurs concurrently with electrolyte oxidation in EC:DMC 1 M LiBOB electrolytes.³⁴

Electrochemical Cycling. To test the viability of the NMP–TMP solvent mixtures with NaBOB salt as the electrolyte system in sodium-ion batteries, we used full cells with hard carbon (HC) anodes and Prussian white (PW) cathodes. Initial cycling was performed at $30 \text{ mA}\cdot\text{g}^{-1}$ (0.2C) for five cycles; after this, cycling progressed at $150 \text{ mA}\cdot\text{g}^{-1}$ (1C) until cycle 52 where a $30 \text{ mA}\cdot\text{g}^{-1}$ current was used for a single cycle to ascertain the amount of capacity recovery at low current. All the reported capacities and C-rates are calculated from the active material weight of the cathode assuming $150 \text{ mAh}\cdot\text{g}^{-1}$ capacity.³⁵ Note that a minimum of three cells was cycled for

each electrolyte formulation to present the variance in the measurements.

During the first formation cycle at 0.2C , the cells with NaBOB–TMP achieved 73% average Coulombic efficiency (CE) while the corresponding value for NaBOB–NMP was 68%. These values can be compared to the 83% CE of the first cycle for the cells using 1 M NaPF_6 in EC:DEC, which is included here as a reference. The mixtures of NMP and TMP yielded CE values that were increasing with TMP content, although the NaBOB–90:10 and NaBOB–80:20 electrolytes performed worse than the pure NaBOB–NMP by a slight margin (see Figure 5a). In full cells, mass balance is an important parameter for the CE, therefore the N/P mass ratio was cross-checked with the CE values for the electrolyte mixtures, and the results show that the differing values between the samples are not caused by mass loading inconsistencies (see Figure S4).

During the subsequent four formation cycles (Figure 5b), the NaBOB–TMP electrolyte showed superior CE compared to the other NMP–TMP-based electrolytes while mixtures between 70:30 and 40:60 displayed worse performance than NaBOB–NMP. Figure 5b shows that all electrolytes except the 50:50 NMP–TMP sample reach a CE above 98% at the end of the fifth formation cycle. There was also a clear trend showing that mixtures close to 50:50 were not effective at passivating the electrodes while electrolytes containing up to 30% of either NMP or TMP performed close to their majority solvent counterpart.

The voltage profiles in Figure 5c–e show the characteristic NaBOB decomposition plateau during the first $20\text{--}25 \text{ mAh}\cdot\text{g}^{-1}$ of charge capacity in the first cycle for electrolytes containing NaBOB, while a more traditional SEI forming region was observed in the reference cell (Figure 5f). When reducing the cycling rate to 0.2C at cycle 52, it can be noted that the cells regain capacity primarily by the mechanism of higher discharge. This holds true for all electrolytes, and thus it indicates that the Prussian White material suffers from over potential during sodiation after extended cycling.

The long-term cycling data collected at a 1C cycling rate reaffirmed that TMP-rich electrolytes were the best in terms of capacity retention (Figure 6a). TMP as the sole solvent and NMP–TMP (10:90) electrolytes preserved more capacity after cycle 1000 than the reference electrolyte, with 57% and 53%

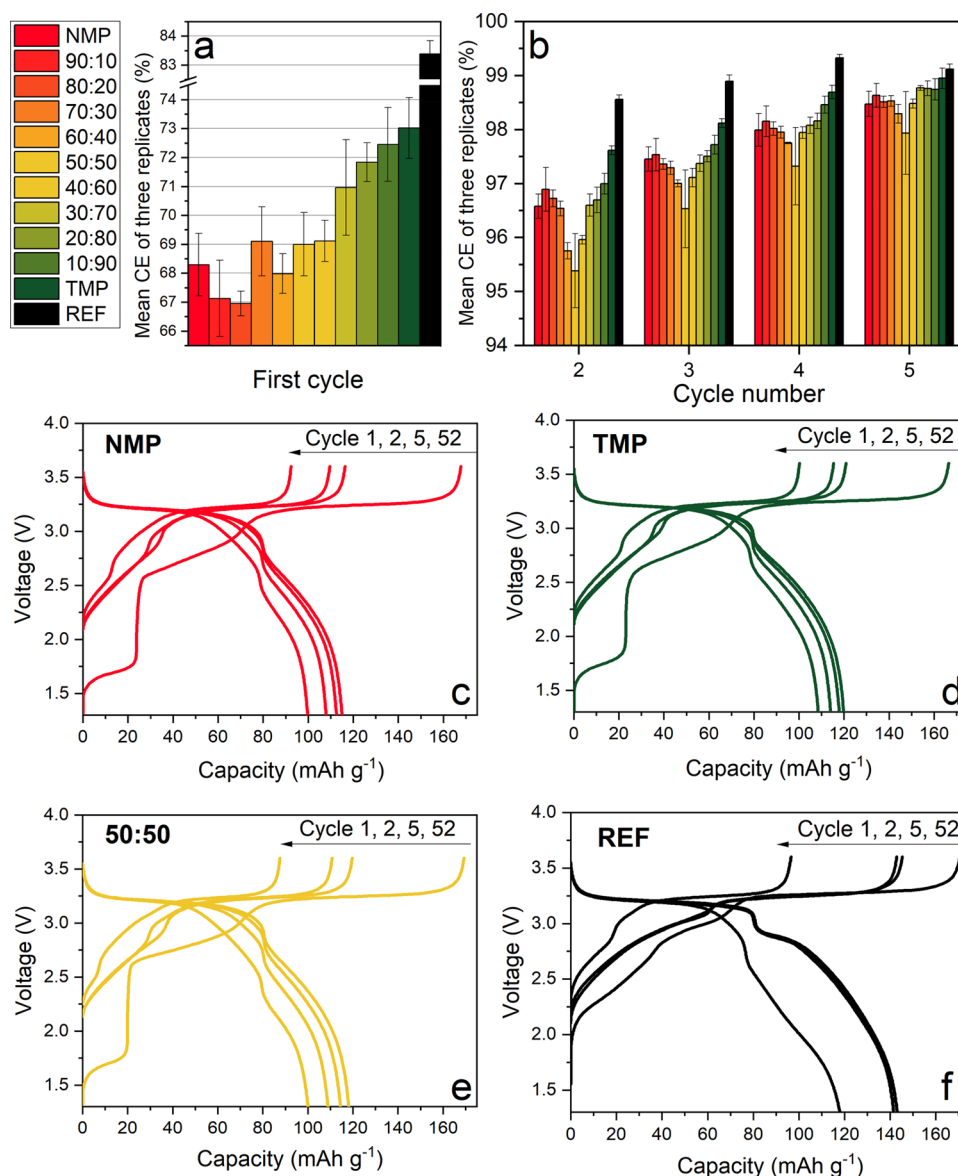


Figure 5. Galvanostatic cycling of full-cell sodium-ion batteries with hard carbon anodes and Prussian white cathodes. The initial average Coulombic efficiency for the first cycle (a) and subsequent four formation cycles (b) of all TMP–NMP electrolytes and the voltage profiles for cycles 1, 2, and 5 as well as the 52th recovery cycle for NaBOB–NMP (c), NaBOB–TMP (d), NaBOB–50:50 (e), and 1 M NaPF₆ in EC:DEC reference cell (f).

retention of the initial discharge capacity for NaBOB–TMP and NaBOB–10:90, respectively, comparing favorably to the 37% retention of the reference cell. The electrolyte based on NMP as the sole solvent retained 49% of the capacity at cycle 1000. The electrolytes containing more than 70% NMP were quite similar as they displayed 41%, 47%, and 40% capacity retention at cycle 1000 for NaBOB–90:10, NaBOB–80:20, and NaBOB–70:30 electrolytes, respectively.

The electrolytes containing 50% or 60% TMP were underperforming in a noticeable manner, and just as in cyclic voltammetry, it seems that mixtures close to 50:50 formed poor passivation layers. The average CE for cycles 10–1000 presented in Figure 6b follows the trend in Figure 6a (a map of CE of individual cycle for all electrolyte is shown in Figure S5).

Rate tests were performed to assess the performance of the electrolytes at different current densities. The measurements consisted of five cycles each at 30, 75, 150, 300, 600, and 1200

mA·g⁻¹ of the cathode material and a subsequent return to 30 mA·g⁻¹ by the same current and cycle increments (see Figure 7). It is apparent that the higher conductivity of NMP-rich mixtures enables better performance above 600 mA·g⁻¹ and the best performing cells in this regard contained 70%–90% NMP. TMP-rich mixtures showed poor performance above 600 mA·g⁻¹, and the irreversible capacity loss caused by the high rates was also markedly greater than for NMP-rich electrolytes. Although we measured only one cell of each composition in this test, the trend is quite clear and shows that NMP is preferred from a rate capability perspective. The reference cell with 1 M NaPF₆ in EC:DEC performed poorly above 300 mA·g⁻¹ but recovered a substantial amount of the lost capacity as the rate was decreased. The rate capability performance of NaBOB compares favorably to that of NaPF₆-based cells, and this is contrary to the experience from the analogue case of LIB electrolytes in combination with LiBOB, where the rate capability is often stated as inferior to more traditional salts.^{36,20}

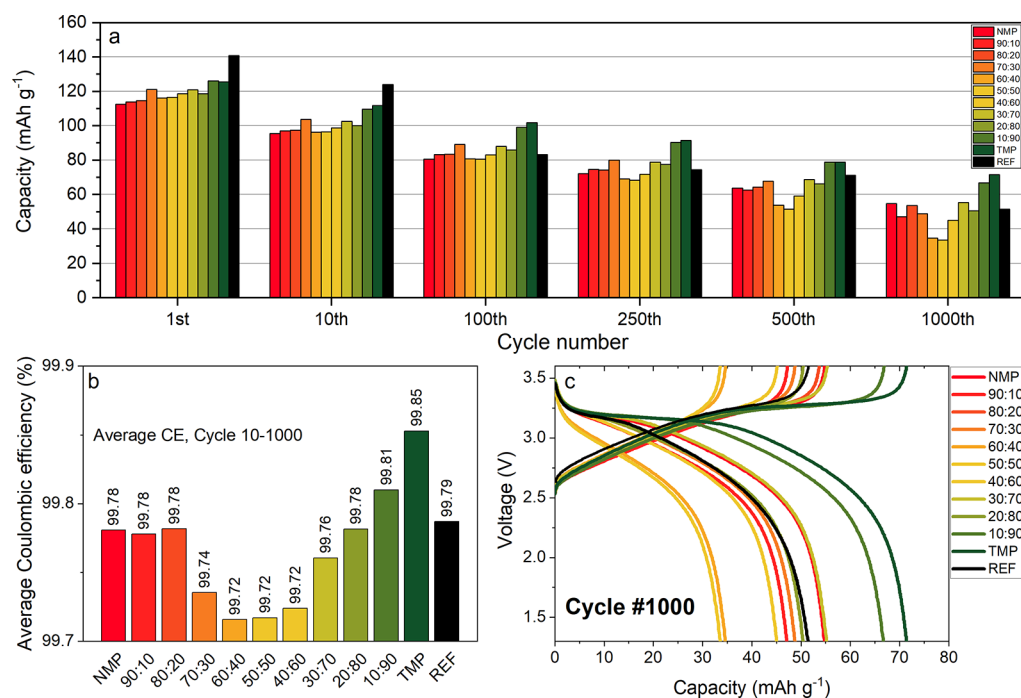


Figure 6. Long-term cycling of full-cell sodium-ion batteries with hard carbon anodes and Prussian white cathodes using different electrolytes. Specific capacity vs cycle number (a), average Coulombic efficiency over cycles 10–1000 (b), and voltage profiles at cycle number 1000 for all electrolyte mixtures (c).

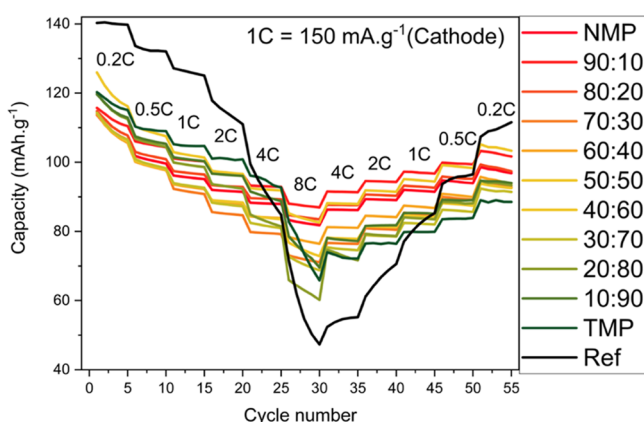


Figure 7. Rate tests of full-cell sodium-ion batteries based on hard carbon anodes and Prussian white cathode using different electrolyte compositions.

Evaluation of the galvanostatic cycling of the cells cycled at 55 °C points out the NaBOB–NMP electrolyte as the best electrolyte candidate for elevated temperature cycling (see Figure 8a). The cell with NaBOB–NMP delivered a capacity retention of 91 mAh.g⁻¹ after 100 cycles at 55 °C compared to 75 mAh.g⁻¹ at room temperature. The cell with NaBOB–TMP electrolytes showed somewhat accelerated capacity fading, while the cell with 1 M NaPF₆ in EC:DEC suffered from a dramatic failure within five cycles. All mixtures of NMP and TMP were underperforming and showed no benefits as compared to the sole solvents. Compared to CE at room temperature, the CE in the initial cycle was 1% lower for NMP at 55 °C while it was 2% higher for both the reference electrolyte and TMP. Although the improved performance of the cell with NaBOB–NMP at elevated temperatures is quite interesting, it should be noted that all electrolytes including NaBOB–NMP showed lower CE

during both 0.2C and 1C cycling than at room temperature (Figure 8b).

The self-discharge of NaBOB–NMP, NaBOB–TMP, and the NaBOB–50:50 electrolytes was determined by extended pause tests at cycle 6 in the fully charged state for cells that were cycled at 0.2C (see Figure 9a).^{37,38} The pause was applied for 100 h, and the lost capacity was determined by comparing the charge capacity of the cycle prior to the pause with the discharge after the pause step as well as with the discharge on the following cycles (*i.e.*, charge capacity of cycle 6 is compared to the discharge in cycles 6 and 7). Although all three samples tested suffered from self-discharge, TMP only lost 11.6% followed by NMP at 20.7% while the 50:50 electrolyte lost 32.4% of its capacity. When comparing the charge capacity prior to the pause to the discharge for the next cycle, *i.e.*, the 7th discharge, we observed that the majority of the capacity loss for NaBOB–TMP was irreversible while approximately half of the capacity loss for NaBOB–NMP and NaBOB–50:50 electrolytes was recoverable. Despite the recovery of capacity, it is clear that NMP and 50:50 mixtures are inferior solvents in terms of static SEI stability by all metrics (Figure 9b,c).

A summary of the strength and weakness of each electrolyte formulation in respect of different requirements is illustrated in Figure 10. The TMP-rich electrolytes provide promising capacity retention at room temperature, nonflammability, and high CE in the first cycle and in long-term cycling. The NMP-rich electrolytes, however, display excellent ionic conductivities and promising rate capability. The electrolytes based on mixtures of TMP and NMP, however, provide low freezing point with high ionic conductivity, which can be useful for specific applications at low temperatures. All these electrolyte mixtures based on NaBOB salt open opportunities to develop fluorine-free electrolyte sodium-ion batteries.

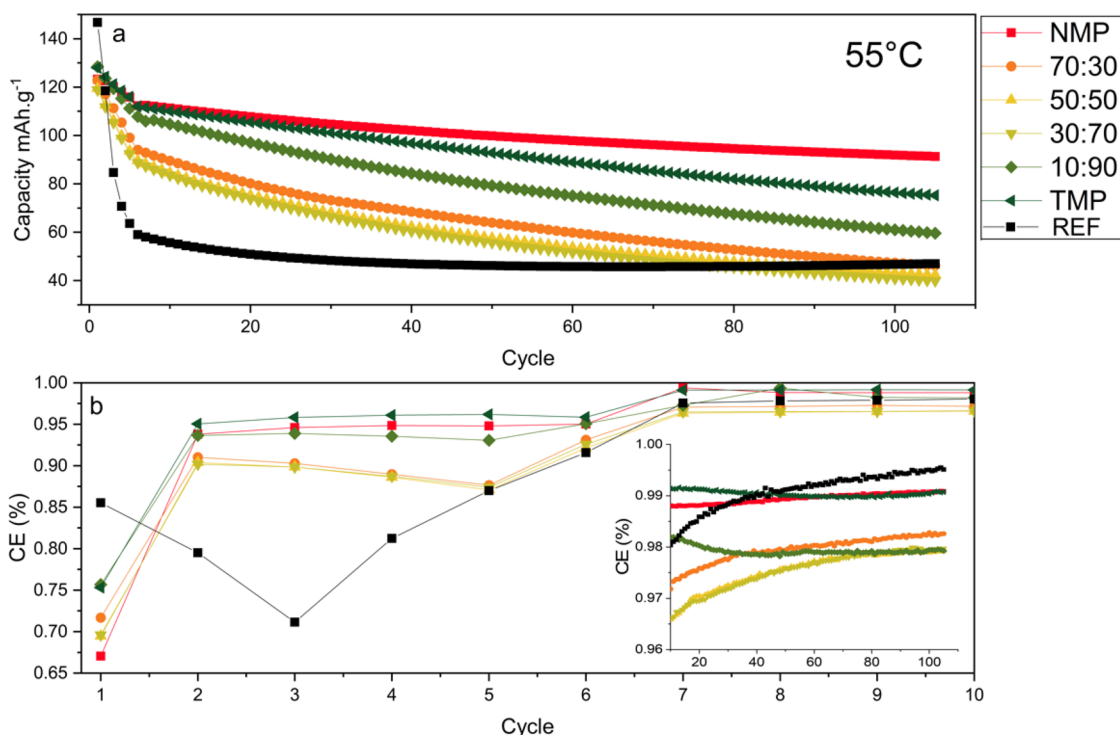


Figure 8. Galvanostatic cycling of full-cell sodium-ion batteries at 55 °C starting with five cycles at 0.2C followed by 100 cycles at 1C (a) and the Coulombic efficiencies for the same cells (b).

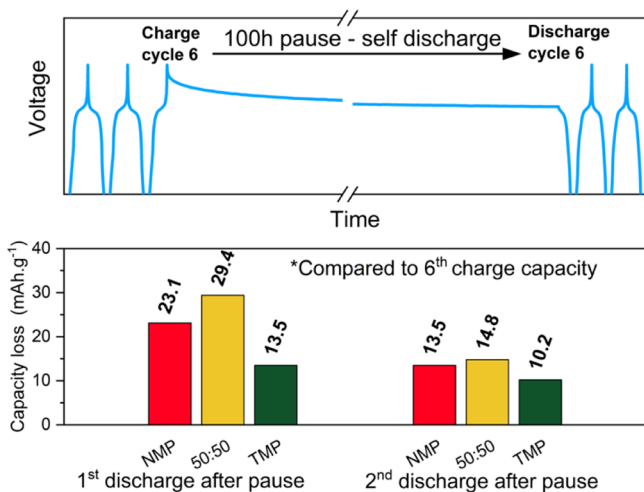


Figure 9. Overview of the extended pause test combined with a galvanostatic cycling program (a) with the capacity loss from the pause in the first and second discharge following the pause displayed in mAh.g⁻¹ (b).

CONCLUSIONS

NaBOB dissolved in NMP, TMP, or their mixtures provide promising electrolytes for sodium-ion battery research. The proposed electrolytes outperform many previously studied electrolytes for sodium-ion batteries in terms of ionic conductivity, high-temperature performance, and having the potential to decrease the electrolyte cost. The studied electrolytes provided promising long-term cycling in full-cell sodium-ion batteries based on hard carbon anodes and Prussian white cathodes. NaBOB–NMP–TMP electrolytes containing less than 30 vol % NMP are nonflammable and share properties

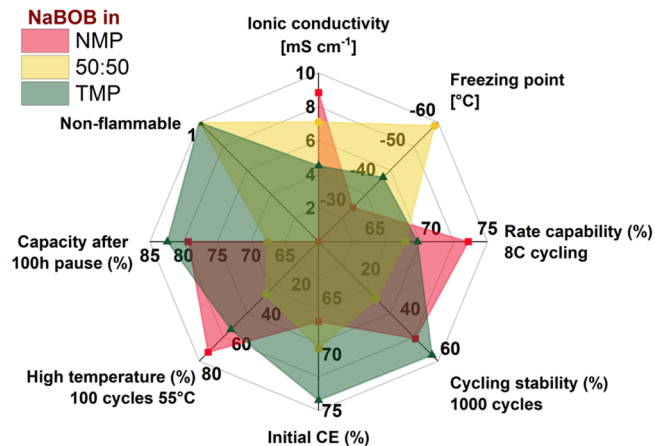


Figure 10. Radar plot comparing TMP–NaBOB, NMP–NaBOB, and TMP–NMP 1:1 NaBOB electrolytes. The figure shows ionic conductivity. Freezing point as determined using the 0.1 mS cm⁻¹ temperature as a threshold. Rate capability is described as the percent remaining capacity in the first discharge at 8C as compared to the initial discharge capacity. Cycling stability and high-temperature performance likewise compare the initial discharge capacity with the capacity at cycles 1000 and 100, respectively.

like good ionic conductivity over a wide temperature range while possessing good high-temperature performance and retaining over 50% capacity over 1000 cycles.

Although all the investigated electrolytes based on NaBOB and NMP–TMP displayed improved electrochemical cycling at 55 °C compared to the cells with the conventional electrolyte of 1 M NaPF₆ in EC:DEC, pure NMP and TMP solvents were most promising. The rate performance of the cells with NMP–NaBOB and NMP–TMP electrolytes compares favorably to that with TMP–NaBOB- and EC:DEC–NaPF₆-based electro-

lytes. However, TMP–NaBOB showed the smallest capacity loss due to self-discharge, decent initial CE, and very good capacity retention in prolonged cycling. Since a battery electrolyte must possess a good balance of many different properties, the conclusion is that NMP addition to TMP can improve conductivity and lower freezing point but any addition above 10 vol % will introduce detrimental effects.

From a pure gravimetric energy density perspective, the performance of the system is approximately 215 Wh kg⁻¹ for NaBOB–NMP, 224 Wh kg⁻¹ for NaBOB–TMP, and 257 Wh kg⁻¹ for EC:DEC 1 M NaPF₆ based on both the anode and cathode active materials in the first cycle. This of course goes to show that the initial Coulombic efficiency is very important and must be improved for NMP and TMP electrolytes.

The low-temperature performance of NMP–TMP mixtures remains to be tested in batteries, but the preservation of acceptable ionic conductivity in what would be the harshest of Scandinavian winter temperatures is very promising for practical application of the electrolyte. The NMP–TMP system is an interesting model system for further development of practical nonflammable electrolytes. This work shows that the benefits of expensive and heavily fluorinated electrolytes such as nonflammability and a wide temperature window can in fact be attained by using low concentrations of NaBOB salt in relatively cheap solvents that also give the added bonus of a practical conductivity.

■ EXPERIMENTAL SECTION

Materials. Trimethyl phosphate (99%) and *N*-methyl-2-pyrrolidone (99.5%) were purchased from Merck and produced by Acros. TMP and NMP were dried over freshly activated molecular sieves before use. NaBOB was synthesized using the method stated by Zavalij *et al.*²¹ with the added step of recrystallizing the synthesized NaBOB in TMP before vacuum drying at 100 degrees over 12 h to make sure that the salt was sufficiently dry for use in an electrolyte. Altris AB supplied Prussian white (PW) cathode powder.

Electrolyte Preparation. All handling and preparation of electrolytes and solvent mixtures were performed in an argon glovebox (O₂, H₂O < 1 ppm) unless otherwise stated. In total, 11 electrolyte samples were prepared, two samples consisting of the pure solvents, and nine NMP–TMP mixtures prepared by mixing the dried solvents based on volume percent. The electrolytes were prepared by slow addition of NaBOB under stirring until the resulting solution remained turbid overnight, whereupon very slight amounts of solvent mixture were very slowly added until the solution turned clear. Weighing of the solutions during the mixing process ensured that the weight percent of salt of the solution was known, and the molarity of electrolytes was obtained by weighing precise volumes of the electrolytes to determine the density.

Flammability Test. The flammability tests were performed on electrolytes using NaBOB concentrations according to their maximum conductivity by soaking a strip of glass fiber in the electrolyte and exposing it to a butane gas flame in a fume hood. The tests were recorded using a mobile phone camera, and pictures and times were collected from recordings.

Analytical Methods. Room temperature conductivity was determined using a Mettler Toledo SevenGo Duo pro pH/ORP/Ion/Conductivity meter SG78 with an InLab 738ISM probe under argon in a glovebox. Cryogenic measurements used the same instrument but were performed in a fume hood by cooling the samples and an aluminum block acting as a thermal buffer with liquid N₂, and the measurements were performed as the sample naturally heated to room temperature. DSC was performed on a TA instruments DSC Q2000 differential scanning calorimeter. The measurements were done between -90 °C and RT with 5 °C/min ramp both for cooling and heating. All sample preparation was performed under an inert atmosphere in a glovebox. The samples were placed in hermetically sealed aluminum pans.

Electrode Preparation and Cell Assembly. For the cathode, Prussian white powder, super C65 (C-ENERGY) carbon additive, and NaCMC binder (Sigma-Aldrich) were mixed in an 85:10:5 wt % ratio, respectively. Approximately 5 mL of distilled water per gram of active material was then added before mixing for 1 h using a planetary ball-mill. The slurry was coated using an applicator rod with a 150 μm gap onto 20 μm carbon-coated aluminum foil. Hard carbon anodes were also prepared on carbon-coated aluminum foil using a 95:5 wt % ratio of hard carbon and NaCMC binder with approximately 6 mL distilled water per gram of active material before mixing for 1 h using planetary ball-mill and coated using a 100 μm-gap applicator rod. The anodes and cathodes were both punched into 20 mm-diameter disks with mass loadings after drying of approximately 1.9 mg/cm² for Prussian white and 1.1 mg/cm² for hard carbon electrodes. The electrodes were dried at 140 °C in vacuum overnight. Whatman glass-fiber separators (30 mm in diameter) and 200 μL of electrolyte were used in pouch cells that were sealed at 2 mBar vacuum. All cell assembly and electrode drying were performed in an argon glovebox.

Electrochemical Methods. The cycling window was set between 1.3 and 3.6 V for all galvanostatic cycling. Galvanostatic cycling and pause tests were performed using a LAND CT2001A battery tester, while the rate tests were performed using a Neware BTS4000 galvanostat. Cycling at 55 °C was performed using a Novonix high precision charger with five formation cycles at 0.2C followed by 100 cycles at 1C. All cells were left to soak for 6 h or more before the start of cycling, and the C-rate was calculated assuming 150 mAh·g⁻¹ capacity for the cathode active material weight.

Cyclic voltammetry was performed on a Biologic MPG2 potentiostat. The measurements were performed in three-electrode pouch cells with Na-metal or with a Prussian white reference electrode desodiated to 3.289 V vs Na⁺/Na. A 13 mm-diameter aluminum foil disk was used as the working electrode, while a 20 mm diameter aluminum foil disk was used as the counter electrode. The scans were performed using a 0.1 mV/s scan speed with scans starting at open circuit voltage. For the oxidation cells, scans were performed between 4.5 and 2 V vs Na⁺/Na. For the reduction cells, scans were performed between 0.01 and 2 V vs Na⁺/Na. For voltammetry, the NaBOB concentrations were 0.66 M for NMP, 0.58 M for 50:50, and 0.42 M for TMP in both reduction and oxidation cells. The currents for the oxidation cells were shifted +3 μA for NMP and +1.5 μA 50:50 for clarity. The voltages in all sweeps have been shifted by 3.289 V to sodium potential in figures corresponding to the potential of the desodiated PW reference electrode vs sodium metal.

■ ASSOCIATED CONTENT

Supporting Information

The Supporting Information is available free of charge at <https://pubs.acs.org/doi/10.1021/acs.chemmater.0c03570>.

Complete DSC scans of all salt-free solvent mixtures and pure solvents, first charge of the studied electrolytes with the total charge capacity, cyclic voltammetry of three-electrode cells to investigate the electrochemical stability window, average Coulombic efficiency and the N/P ratio of active mass in the electrode (black) for all the NMP–TMP electrolytes, and Coulombic efficiencies for cycles 6–1000 of all long-term cycled cells (PDF)

Flammability test of the NMP–TMP 90:10 electrolyte (MP4)

Flammability test of the NMP–TMP 80:20 electrolyte (MP4)

Flammability test of the NMP–TMP 70:30 electrolyte (MP4)

Flammability test of the NMP–TMP 60:40 electrolyte (MP4)

Flammability test of the NMP–TMP 50:50 electrolyte (MP4)

Flammability test of the NMP–TMP 40:60 electrolyte (MP4)

Flammability test of the NMP–TMP 30:70 electrolyte (MP4)

Flammability test of the NMP–TMP 20:80 electrolyte (MP4)

Flammability test of the NMP–TMP 10:90 electrolyte (MP4)

Flammability test of the pure TMP electrolyte (MP4)

AUTHOR INFORMATION

Corresponding Author

Reza Younesi – Department of Chemistry-Ångström Laboratory, Uppsala University, Uppsala SE-75121, Sweden; orcid.org/0000-0003-2538-8104; Email: reza.younesi@kemi.uu.se

Authors

Ronnie Mogensen – Department of Chemistry-Ångström Laboratory, Uppsala University, Uppsala SE-75121, Sweden

Alexander Buckel – Department of Chemistry-Ångström Laboratory, Uppsala University, Uppsala SE-75121, Sweden

Simon Colbin – Department of Chemistry-Ångström Laboratory, Uppsala University, Uppsala SE-75121, Sweden

Complete contact information is available at:

<https://pubs.acs.org/10.1021/acs.chemmater.0c03570>

Notes

The authors declare the following competing financial interest(s): The Prussian white powder used as positive electrode material in this study was provided by ALTRIS AB, a company founded by R.M and R.Y. The other authors in this paper declare to have no competing interests.

ACKNOWLEDGMENTS

We would like to thank ÅForsk Foundation via grants nos. 1907-2009 and 20-675, the Swedish Energy Agency via grant nos. 50177-1 and 48198-1, and STandUP for Energy for the financial support.

REFERENCES

- (1) Pan, H.; Hu, Y.-S.; Chen, L. Room-temperature stationary sodium-ion batteries for large-scale electric energy storage. *Energy Environ. Sci.* **2013**, *6*, 2338.
- (2) Hwang, J.-Y.; Myung, S.-T.; Sun, Y.-K. Sodium-ion batteries: present and future. *Chem. Soc. Rev.* **2017**, *46*, 3529–3614.
- (3) Vaalma, C.; Buchholz, D.; Weil, M.; Passerini, S. A cost and resource analysis of sodium-ion batteries. *Nat. Rev. Mater.* **2018**, *3*, 18013.
- (4) Mogensen, R.; Colbin, S.; Younesi, R. An attempt to formulate non-carbonate electrolytes for sodium-ion batteries. *Batteries Supercaps* **2020**, DOI: [10.1002/batt.202000252](https://doi.org/10.1002/batt.202000252)
- (5) Monti, D.; et al. Towards standard electrolytes for sodium-ion batteries: physical properties, ion solvation and ion-pairing in alkyl carbonate solvents. *Phys. Chem. Chem. Phys.* **2020**, *22*, 22768–22777.
- (6) Liu, T.; et al. Exploring competitive features of stationary sodium ion batteries for electrochemical energy storage. *Energy Environ. Sci.* **2019**, *12*, 1512–1533.
- (7) Xu, W.; Angell, C. A. Weakly Coordinating Anions, and the Exceptional Conductivity of Their Nonaqueous Solutions. *Electrochem. Solid-State Lett.* **2001**, *4*, E1.
- (8) Xu, K.; Zhang, S. S.; Lee, U.; Allen, J. L.; Jow, T. R. LiBOB: Is it an alternative salt for lithium ion chemistry? *J. Power Sources* **2005**, *146*, 79–85.

(9) Renner, R. Growing concern over perfluorinated chemicals. *Environ. Sci. Technol.* **2001**, *35*, 154A–160A.

(10) Mogensen, R.; Colbin, S.; Menon, A. S.; Björklund, E.; Younesi, R. Sodium Bis(oxalato)borate in Trimethyl Phosphate: A Fire-Extinguishing, Fluorine-Free, and Low-Cost Electrolyte for Full-Cell Sodium-Ion Batteries. *ACS Appl. Energy Mater.* **2020**, *3*, 4974–4982.

(11) Xu, K.; Zhang, S.; Jow, T. R.; Xu, W.; Angell, C. A. LiBOB as Salt for Lithium-Ion Batteries: A Possible Solution for High Temperature Operation. *Electrochem. Solid-State Lett.* **2002**, *5*, A26.

(12) Yu, B. T.; Qiu, W. H.; Li, F. S.; Xu, G. X. The electrochemical characterization of lithium bis(oxalato)borate synthesized by a novel method. *Electrochem. Solid-State Lett.* **2006**, *9*, A1.

(13) Jin, T.; et al. Nonflammable, Low-Cost, and Fluorine-Free Solvent for Liquid Electrolyte of Rechargeable Lithium Metal Batteries. *ACS Appl. Mater. Interfaces* **2019**, *11*, 17333–17340.

(14) Hernández, G.; et al. Elimination of Fluorination: The Influence of Fluorine-Free Electrolytes on the Performance of LiNi 1/3 Mn 1/3 Co 1/3 O 2 /Silicon–Graphite Li-Ion Battery Cells. *ACS Sustainable Chem. Eng.* **2020**, *8*, 10041–10052.

(15) Valvo, M.; Liivat, A.; Eriksson, H.; Tai, C. W.; Edström, K. Iron-Based Electrodes Meet Water-Based Preparation, Fluorine-Free Electrolyte and Binder: A Chance for More Sustainable Lithium-Ion Batteries? *ChemSusChem* **2017**, *10*, 2431–2448.

(16) Huang, J.-Y.; et al. Study on γ -butyrolactone for LiBOB-based electrolytes. *J. Power Sources* **2009**, *189*, 458–461.

(17) Li, S.; Xue, Y.; Cui, X.; Geng, S.; Huang, Y. Effect of sulfolane and lithium bis(oxalato)borate-based electrolytes on the performance of spinel LiMn₂O₄ cathodes at 55°C. *Ionics* **2016**, *22*, 797–801.

(18) Feng, J. K.; Ai, X. P.; Cao, Y. L.; Yang, H. X. Possible use of non-flammable phosphonate ethers as pure electrolyte solvent for lithium batteries. *J. Power Sources* **2008**, *177*, 194–198.

(19) Xu, K.; Zhang, S.; Poesse, B. A.; Jow, T. R. Lithium bis(oxalato)borate stabilizes graphite anode in propylene carbonate. *Electrochem. Solid-State Lett.* **2002**, *5*, A259.

(20) Kaneko, H.; Sekine, K.; Takamura, T. Power capability improvement of LiBOB/PC electrolyte for Li-ion batteries. *J. Power Sources* **2005**, *146*, 142–145.

(21) Zavalij, P. Y.; Yang, S.; Whittingham, M. S. Structures of potassium, sodium and lithium bis(oxalato)borate salts from powder diffraction data. *Acta Crystallogr. Sect. B Struct. Sci.* **2003**, *59*, 753–759.

(22) Wang, L.; et al. Functionalized Carboxyl Carbon/NaBOB Composite as Highly Conductive Electrolyte for Sodium Ion Batteries. *ChemistrySelect* **2018**, *3*, 9293–9300.

(23) Zeng, Z.; et al. A Safer Sodium-Ion Battery Based on Nonflammable Organic Phosphate Electrolyte. *Adv. Sci.* **2016**, *3*, 1600066.

(24) Rudola, A.; Du, K.; Balaya, P. Monoclinic Sodium Iron Hexacyanoferrate Cathode and Non-Flammable Glyme-Based Electrolyte for Inexpensive Sodium-Ion Batteries. *J. Electrochem. Soc.* **2017**, *164*, A1098–A1109.

(25) Goodenough, J. B.; Kim, Y. Challenges for Rechargeable Li Batteries. *Chem. Mater.* **2010**, *22*, 587–603.

(26) Jiang, X.; et al. An All-Phosphate and Zero-Strain Sodium-Ion Battery Based on Na₃V₂(PO₄)₃ Cathode, NaTi₂(PO₄)₃ Anode, and Trimethyl Phosphate Electrolyte with Intrinsic Safety and Long Lifespan. *ACS Appl. Mater. Interfaces* **2017**, *9*, 43733–43738.

(27) Liu, X.; et al. High Capacity and Cycle-Stable Hard Carbon Anode for Nonflammable Sodium-Ion Batteries. *ACS Appl. Mater. Interfaces* **2018**, *10*, 38141–38150.

(28) Wang, J.; et al. Fire-extinguishing organic electrolytes for safe batteries. *Nat. Energy* **2018**, *3*, 22–29.

(29) Liu, X.; et al. High-Safety Symmetric Sodium-Ion Batteries Based on Nonflammable Phosphate Electrolyte and Double Na₃V₂(PO₄)₃ Electrodes. *ACS Appl. Mater. Interfaces* **2019**, *11*, 27833–27838.

(30) Cao, R.; et al. Enabling room temperature sodium metal batteries. *Nano Energy* **2016**, *30*, 825–830.

(31) Wypych, A.; Wypych, G. *Databook of Green Solvents*; ChemTec Publishing, 2014, 1–600.

- (32) Lisicki, Z.; Jamróz, M. E. (Solid + liquid) equilibria in (polynuclear aromatic + tertiary amide) systems. *J. Chem. Thermodyn.* **2000**, *32*, 1335–1353.
- (33) Knill, C. J.; Kennedy, J. F. CRC handbook of data on organic compounds. *Carbohydr. Polym.* **1995**, *26*, 243.
- (34) Zhang, X.; Devine, T. M. Passivation of Aluminum in Lithium-Ion Battery Electrolytes with LiBOB. *J. Electrochem. Soc.* **2006**, *153*, B365.
- (35) Brant, W. R.; et al. Selective Control of Composition in Prussian White for Enhanced Material Properties. *Chem. Mater.* **2019**, *31*, 7203–7211.
- (36) Yu, B. T.; Qiu, W. H.; Li, F. S.; Cheng, L. Comparison of the electrochemical properties of LiBOB and LiPF₆ in electrolytes for LiMn₂O₄/Li cells. *J. Power Sources* **2007**, *166*, 499–502.
- (37) Ma, L. A.; Naylor, A. J.; Nyholm, L.; Younesi, R. Strategies of mitigating dissolution of solid electrolyte interphases in sodium-ion batteries. *Angew. Chem., Int. Ed.* **2021**, *60*, 2–11.
- (38) Mogensen, R.; Brandell, D.; Younesi, R. Solubility of the Solid Electrolyte Interphase (SEI) in Sodium Ion Batteries. *ACS Energy Lett.* **2016**, *1*, 1173–1178.